

# Physical analysis of an acrylic resin modified by metal and ceramic nanoparticles

Luciana Machado-Santos<sup>1,A-D,F</sup>, Kusai Baroudi<sup>1,2,A,B,E,F</sup>, Nikolaos Silikas<sup>3,A-D,F</sup>, João Paulo Mendes Tribst<sup>4,C-F</sup>, Mario Alexandre Coelho Sinhoreti<sup>5,A,B,D,F</sup>, William Cunha Brandt<sup>6,A-D</sup>, Priscila Christiane Suzy Liporoni<sup>1,A,B,D,F</sup>

<sup>1</sup> Department of Restorative Dentistry, School of Dentistry, University of Taubaté, Brazil

<sup>2</sup> RAK College of Dental Sciences, RAK Medical and Health Sciences University, Ras Al Khaimah, UAE

<sup>3</sup> Department of Dentistry, School of Medical Sciences, University of Manchester, UK

<sup>4</sup> Department of Reconstructive Oral Care, Academic Centre for Dentistry Amsterdam (ACTA), Universiteit van Amsterdam and Vrije Universiteit Amsterdam, Amsterdam, the Netherlands

<sup>5</sup> Department of Dental Materials, Piracicaba Dental School, State University of Campinas, Brazil

<sup>6</sup> Department of Dentistry, University of Santo Amaro, São Paulo, Brazil

A – research concept and design; B – collection and/or assembly of data; C – data analysis and interpretation; D – writing the article; E – critical revision of the article; F – final approval of the article

Dental and Medical Problems, ISSN 1644-387X (print), ISSN 2300-9020 (online)

Dent Med Probl. 2023;60(4):657–664

## Address for correspondence

João Paulo Mendes Tribst  
E-mail: joao.tribst@gmail.com

## Funding sources

None declared

## Conflict of interest

None declared

## Acknowledgements

None declared

Received on July 21, 2023

Reviewed on August 29, 2023

Accepted on September 4, 2023

Published online on November 15, 2023

## Cite as

Machado-Santos L, Baroudi K, Silikas N, et al. Physical analysis of an acrylic resin modified by metal and ceramic nanoparticles. *Dent Med Probl.* 2023;60(4):657–664. doi:10.17219/dmp/171844

## DOI

10.17219/dmp/171844

## Copyright

Copyright by Author(s)

This is an article distributed under the terms of the Creative Commons Attribution 3.0 Unported License (CC BY 3.0) (<https://creativecommons.org/licenses/by/3.0/>).

## Abstract

**Background.** Nanoparticles (NPs) have gained significant attention in various fields due to their unique properties and potential applications. Polymethyl methacrylate (PMMA) is an acrylic resin widely used in dentistry and medicine. However, the effect of different types of NP fillers on the physical properties of PMMA-based resins has not been thoroughly explored in the literature.

**Objectives.** The present study aimed to evaluate the effects of 3 different types of NP fillers on the physical properties of an experimental PMMA-based resin as a function of the NP content and concentration.

**Material and methods.** Ten groups ( $n = 10$ ) were designed. The specimens were composed of an acrylic resin, silicon dioxide ( $\text{SiO}_2$ ), cerium dioxide ( $\text{CeO}_2$ ), and titanium dioxide ( $\text{TiO}_2$ ) at the following ratios (wt%): group 1 (G1) – control; group 2 (G2) – 0.5%  $\text{SiO}_2$ ; group 3 (G3) – 1%  $\text{SiO}_2$ ; group 4 (G4) – 3%  $\text{SiO}_2$ ; group 5 (G5) – 0.5%  $\text{CeO}_2$ ; group 6 (G6) – 1%  $\text{CeO}_2$ ; group 7 (G7) – 3%  $\text{CeO}_2$ ; group 8 (G8) – 0.5%  $\text{TiO}_2$ ; group 9 (G9) – 1%  $\text{TiO}_2$ ; and group 10 (G10) – 3%  $\text{TiO}_2$ . Transmission electron microscopy (TEM) was used to assess the quality of NP dispersion. Thermal stability was assessed with thermogravimetric analysis (TGA) and differential scanning calorimetry (DSC). The effects of the abovementioned NPs on the properties of the resin were evaluated using the Archimedes principle for density, the Vickers hardness (VH) test and the impact strength (IS) test. Data analysis employed the one- and two-way analysis of variance (ANOVA), followed by Duncan's post hoc test at a significance level of 0.05.

**Results.** Transmission electron microscopy showed partial NP dispersion. All types of NPs enhanced the mechanical properties of the acrylic resin except for IS, which was similar to that of the control group. Among the types of NPs, irrespective of the weight percentage,  $\text{CeO}_2$  showed higher thermal stability and higher IS for 0.5 wt% and 1 wt% as compared to other groups, as well as the highest values of density at 0.5 wt%, 1 wt% and 3 wt%. Titanium oxide at 1 wt% presented a higher VH as compared to other groups. The fracture pattern was the same for all groups.

**Conclusions.** Incorporating the tested NPs into the acrylic resin resulted in enhanced physical properties, primarily attributed to a lower NP content.

**Keywords:** nanoparticles, silicon dioxide, cerium dioxide, titanium dioxide, polymethyl methacrylate

## Introduction

Acrylic resins have been used in dentistry and medicine since 1936, and have remained the primary material for manufacturing dental and craniofacial prostheses.<sup>1</sup> The material is typically fabricated with the use of polymethyl methacrylate (PMMA). The polymer has beneficial biological properties, as it is tasteless, insoluble and compatible with oral tissues. The favorable physical characteristics of PMMA include dimensional stability, resilience, resistance to compression, the ease of handling, and a low cost.<sup>2</sup> However, PMMA is not an ideal material in terms of mechanical properties required for long-term clinical use, such as flexural strength, hardness, density, and thermal stability.<sup>3,4</sup>

To improve the physical properties of different dental biomaterials, composites have been reinforced with inorganic nanofillers.<sup>5–7</sup> Studies have shown that decreasing the size of the reinforcement particles to a nanoscale can completely alter the way they interact with the matrix, either due to the increased surface area or the possible interactions with the matrix in the molecular sphere, changing the chemical characteristics of the matrix.<sup>8</sup>

Silicate-based minerals, such as silica (silicon dioxide (SiO<sub>2</sub>), approx. 40 nm), have been used as inorganic fillers in methacrylate-based resins, and are associated with good mechanical and polishing properties. Numerous studies have demonstrated the correlation between the quantity of silica and the modulus of elasticity, wear resistance and polymerization shrinkage.<sup>9–11</sup>

A previous study incorporated 3 different metal oxides in different proportions into PMMA, namely titania (titanium dioxide (TiO<sub>2</sub>)), zirconium dioxide (ZrO<sub>2</sub>) and aluminum oxide (Al<sub>2</sub>O<sub>3</sub>), and concluded that all experimental groups showed better resistance to impact, sorption and solubility as compared to the control group.<sup>3</sup> Cerium-based metallic material, such as ceria (cerium dioxide (CeO<sub>2</sub>)), is transparent to visible light, can act as a catalyst, and has been linked to better compression resistance properties and thermal expansion values of ceramics.<sup>12</sup> Ceria has demonstrated antibacterial properties against *Pseudomonas aeruginosa* after being treated with polyacrylic acid.<sup>13</sup> However, there are no reports on the use of the material in the reinforcement of acrylic resins.

Titanium dioxide nanoparticles (NPs) are chemically inert, resistant to corrosion, non-toxic, and inexpensive. They have a high refractive index and antibacterial properties under a variety of spectra.<sup>14</sup> For these and other characteristics, TiO<sub>2</sub> NPs are incorporated into polymeric materials, such as PMMA.<sup>15</sup> In comparison with its larger particle version, TiO<sub>2</sub> NPs primarily offer heat stability, clearly define the color of the polymer and provide improved reinforcing properties. As such, the particles do not lose their features during the polymerization process at high temperatures, contributing to the control of polymerization shrinkage.<sup>3</sup> The existing studies indicate that

incorporating surface-treated TiO<sub>2</sub> into a PMMA matrix leads to a reduced shrinkage stress of the polymeric matrix, which is due to the formation of agglomerates that serve as concentration points for these stresses.<sup>16</sup> According to a study by Acosta-Torres et al., with regard to the physical properties of conventional and nanopigmented PMMA, the matrices containing TiO<sub>2</sub> show less porosity.<sup>17</sup> However, certain studies have highlighted the adverse effects associated with incorporating TiO<sub>2</sub> and SiO<sub>2</sub> into polymeric materials.<sup>18,19</sup>

In light of the current literature,<sup>1–19</sup> there is a notable research gap regarding the effects of 3 distinctive NPs – SiO<sub>2</sub>, CeO<sub>2</sub> and TiO<sub>2</sub> – as potential fillers for experimental PMMA-based resins. While the use of NPs as additives has been explored in various materials, their interactions with PMMA-based resins remain surprisingly underrepresented in the current research. Therefore, the present study aimed to bridge this gap by conducting a comprehensive analysis of the influence of these NPs on the mechanical properties of a resin across a spectrum of concentrations. Our study encompassed a thorough examination of density, Vickers hardness (VH) and impact strength (IS) to assess the mechanical behavior of the resin. Furthermore, the study evaluated the thermal stability of the NP-integrated resin via thermogravimetric analysis (TGA) and differential scanning calorimetry (DSC).

The purpose of the present study was to investigate the influence of different content and concentration of SiO<sub>2</sub>, CeO<sub>2</sub> and TiO<sub>2</sub> on the physicochemical properties of an PMMA-based resin. The present hypothesis is that the incorporation of NPs does not alter the properties of PMMA.

## Material and methods

To investigate the effects of different NPs on the properties of a PMMA-based resin, 100 samples ( $N = 100$ ) were prepared and divided into 10 distinct groups ( $n = 10$  per group). A commercially available acrylic resin (Acron™ MC; GC America Inc., Alsip, USA) composed of powder and liquid was used. Three types of NPs, ranging in size from 15 nm to 50 nm, were added to the powder before the polymerization procedure by using a Hauschild SpeedMixer® DAC 150.1 (Hauschild & Co., Hamm, Germany) at 50/60 Hz and 3,500 rpm. The NPs comprised SiO<sub>2</sub> (15 nm), CeO<sub>2</sub> (25 nm) and TiO<sub>2</sub> (50 nm) in standardized sizes, as provided by the manufacturer (SkySpring Nanomaterials Inc., Houston, USA). The specimens in each group were composed of an acrylic resin, SiO<sub>2</sub>, CeO<sub>2</sub>, and TiO<sub>2</sub> at the following ratios (wt%): group 1 (G1) – control; group 2 (G2) – 0.5% SiO<sub>2</sub>; group 3 (G3) – 1% SiO<sub>2</sub>; group 4 (G4) – 3% SiO<sub>2</sub>; group 5 (G5) – 0.5% CeO<sub>2</sub>; group 6 (G6) – 1% CeO<sub>2</sub>; group 7 (G7) – 3% CeO<sub>2</sub>; group 8 (G8) – 0.5% TiO<sub>2</sub>; group 9 (G9) – 1% TiO<sub>2</sub>; and group 10 (G10) – 3% TiO<sub>2</sub>.

The preliminary test using transmission electron microscopy (TEM) suggested that the NPs had better dispersion when added to the powder instead of the liquid. After microwave polymerization, the samples were cut with a vitreous fragment at 45°, and then an ultramicrotome (EM UC6; Leica Microsystems, Wetzlar, Germany) was used to obtain ultrathin (80-nanometer) sections. The slices were placed in a fine mesh (grid storage box; Agar Scientific Ltd., Stansted, UK) and observed under a TEM at 300 Kv (Tecnai G2 F30; FEI Company, Hillsboro, USA) to identify the NP content. The NPs were incorporated into the powder, and the flask was closed and placed inside the mixer at 2,000 rpm for 3 min, then rested on the bench for another 3 min. The liquid was added to the mixture and stirred at 500 rpm for 1 min to prevent the premature packing of the resin, which may occur due to the agitation and shear forces generated during this step. The liquid needs to be thoroughly and evenly dispersed within the powder to achieve a consistent resin.

The size of the samples depended on the specific characteristics of the respective tests. For instance, disk-shaped samples measuring 5 mm × 4 mm were employed in the VH test, while samples measuring 65 mm × 10 mm × 2 mm were utilized for the Charpy IS test. Similarly, the sample mass for TGA was standardized at 20 ± 2 mg. By adjusting the sample sizes according to the unique demands of each test, we aimed to obtain reliable and comprehensive data that would accurately reflect the properties under investigation. However, the inclusion and polymerization processes were standardized for all samples.

Metal molds were used for the TEM and Charpy IS test samples, and composite resin molds were used for all other tested samples. The molds were invested individually with laboratory silicone (Titanium Zetalabor; Zhermack, Badia Polesine, Italy) and covered with type III dental stone (Scola-cast powder; Scola, Cheshire, UK) in a ceramic muffle oven (GC Europe, Leuven, Belgium). The experimental acrylic resin was prepared as previously described and immediately packed into the silicone index at its dough stage. The flasks were slowly and gradually pressed in a hydraulic press until establishing 1.25 kg, and then polymerized in a microwave oven (Daewoo KQG-6L6B, 800 W maximum power; Daewoo Electronics, Wokingham, UK) for 10 min: phase 1 – 3 min at 40% power; phase 2 – 4 min at 0% power; and phase 3 – 3 min at 90% power. Then, the flasks were placed on the bench until completely cooled. The samples were deflasked and their surfaces were smoothed with an electric minigrinder (Dremel® 3000; Robert Bosch Tool Corporation, Mount Prospect, USA) at 5,000–33,000 rpm. For the VH test, one side of the sample was polished with 600–1,200 grit silicon carbide sandpaper (Jiangsu Jianda Grinding Technology Co. Ltd., Wuxi, China). The samples were stored dry at 24 ± 1°C for 24 ± 2 h before the tests.

A sample from each group was submitted for TGA. Thermal stability was determined by means of the thermogravimetric trace record (STARe software; Mettler-Toledo, Greifensee, Switzerland) in an atmosphere of nitrogen (N), using small sample fragments. A heating rate of 10°C/min, with a temperature ranging from 35°C to 600°C, and a sample portion weighing 20 ± 2 mg were used for this test. The balance arm was held in a horizontal reference position and changes in the sample mass caused the beam to bend, which was detected by the photoelectric cells. The TGA curve was obtained by recording variations in temperature and the sample mass continuously. Differential scanning calorimetry was conducted simultaneously with the TGA test, and was used to better understand the thermal behavior and homogeneity of the experimental resin samples. The same fragment from each group (20 ± 2 mg) was analyzed to compare the glass transition temperature ( $T_g$ ) of the polymer (control) and of the NP-modified polymer.

One hundred disk-shaped samples, divided into 10 groups ( $n = 10$  per group), measuring 5 mm × 4 mm and with the top surfaces polished, were evaluated for VH in a microhardness tester (FM-700; Future-Tech Corp., Kawasaki, Japan). A 100-gram load was applied to the polished surface of the sample at the speed of 0.05 mm/s for 10 s, and the values were recorded in Vickers pyramid numbers (HV). Three indentations were made in each sample. Then, the Archimedes principle was applied to investigate density changes, with the mass ( $m$ ) measured on an analytical precision scale and the volume ( $V$ ) determined by the principle. The density of the sample ( $\rho$ ) was calculated using the following formula (Equation 1):

$$\rho = m/V \quad (1)$$

where:

$\rho$  – density [g/cm<sup>3</sup>];

$m$  – mass [g]; and

$V$  – volume [cm<sup>3</sup>].

One hundred samples, divided into 10 groups ( $n = 10$  per group), measuring 65 mm × 10 mm × 2 mm were subjected to the IS test in the Charpy system (Otto Wolpert-Werke, Ludwigshafen am Rhein, Germany) with an impact load of 40 kpcm. The impact load recorderd at the moment of specimen failure was changed to the IS value [kgf/cm<sup>2</sup>] using the following formula (Equation 2):

$$IS = I/L \times H \quad (2)$$

where:

IS – impact strength [kgf/cm<sup>2</sup>];

$I$  – impact load (kpcm);

$L$  – sample length in the impact region [cm]; and

$H$  – sample height in the impact region [cm].

A fractographic analysis was conducted for the 2 sample fragments obtained in the IS test, and a macroscopic analysis was done by the visual inspection of the fractured surfaces, using a claw-mounted magnifier (Western 9051L; Western Ophthalmics Corp., São Paulo, Brazil) at  $\times 4$  magnification. The fragments of each specimen were called fragment A (FA) and fragment B (FB). During visual inspection, when FA and FB could be repositioned at the fracture line, presenting a smooth surface, the fractures were classified as brittle. Those presenting plastic deformation, or exhibiting rough and jagged surfaces were recorded as intermediate (ductile-to-brittle transition) fractures. The fractographic examination verified that all samples could have FA and FB perfectly placed together, and not even the fracture line could be seen at  $\times 4$  magnification; therefore, all samples were classified as brittle. The control and the 1 wt% experimental samples were covered with a fine layer of gold, using a sputter coater (Emitech K550X; Quorum Technologies Ltd., Ashford, UK) and observed under a scanning electron microscope (SEM) (EVO MA10; Carl Zeiss, Oberkochen, Germany) to analyze and compare the fracture morphology and microstructure.

## Statistical analysis

Data analysis employed the one- and two-way analysis of variance (ANOVA), followed by Duncan's post hoc test at a significance level of 0.05.

## Results

Transmission electron microscopy showed enhanced dispersion when NPs were incorporated into the powder component of the acrylic resin. However, the incorporation

method did not completely prevent the formation of agglomerates (Fig. 1). Furthermore, a strong bond between the NPs and the matrix was evident in cases of effective dispersion, while regions with more pronounced agglomeration displayed voids (Fig. 1).

Table 1 presents the TGA and DSC values from the respective thermographs. The curve profiles in both analyses exhibited pattern similarity, displaying only slight temperature shifts. The control group displayed a relatively higher mass loss following the initial event, and preliminary observations suggested that 1% TiO<sub>2</sub> exhibited a relatively higher initial degradation temperature ( $T_i$ ). Moreover, all ceria groups presented higher  $T_i$  values than the control group. The final residue percentage increased proportionally to the amount of incorporated NPs in each group, except for the control group. In the 2<sup>nd</sup> significant mass loss event, the control group

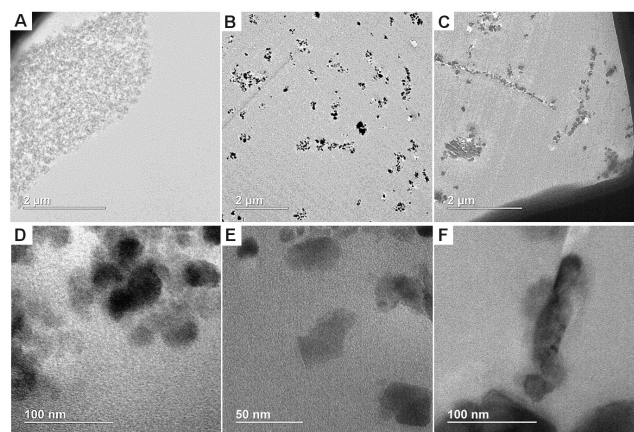


Fig. 1. Transmission electron microscopy (TEM) micrographs showing the dispersion of the nanoparticles (NPs) (3 wt%) within the polymeric matrix (A–C) and the TEM observations of the NP (3 wt%)–matrix bonded interface (D–F). A – silicon dioxide (SiO<sub>2</sub>); B – cerium dioxide (CeO<sub>2</sub>); C – titanium dioxide (TiO<sub>2</sub>); D – SiO<sub>2</sub>; E – CeO<sub>2</sub>; F – TiO<sub>2</sub>.

Table 1. Resin decomposition temperatures, mass loss (ML), residue, and glass transition temperature ( $T_g$ )

Groups	Thermal degradation event						Residue at 600°C [%]	$T_g$ [°C]
	1 <sup>st</sup>			2 <sup>nd</sup>				
	$T_i$ [°C]	$T_{\text{midpoint}}$ [°C]	ML [%]	$T_i$ [°C]	$T_{\text{midpoint}}$ [°C]	ML [%]		
G1	194.46	288.94	13.48	332.63	373.78	84.17	2.36	102.50
G2	195.73	286.40	12.36	328.29	370.95	85.56	2.08	112.50
G3	187.44	286.84	11.01	327.07	372.90	86.52	2.46	105.20
G4	174.37	291.62	11.02	329.49	370.65	84.82	4.15	108.25
G5	198.08	289.51	11.00	329.40	375.20	86.74	2.25	112.50
G6	212.73	297.34	10.10	332.35	375.37	87.03	2.87	107.00
G7	203.09	296.61	8.95	330.12	374.20	86.63	4.42	106.50
G8	198.71	289.95	11.78	328.27	372.66	85.80	2.42	110.50
G9	218.43	296.14	8.97	328.43	372.45	88.03	2.99	109.50
G10	177.47	289.74	13.37	328.61	371.52	82.07	4.56	104.50

Groups: G1 – control; G2 – 0.5% SiO<sub>2</sub>; G3 – 1% SiO<sub>2</sub>; G4 – 3% SiO<sub>2</sub>; G5 – 0.5% CeO<sub>2</sub>; G6 – 1% CeO<sub>2</sub>; G7 – 3% CeO<sub>2</sub>; G8 – 0.5% TiO<sub>2</sub>; G9 – 1% TiO<sub>2</sub>; and G10 – 3% TiO<sub>2</sub>.  $T_i$  – initial degradation temperature;  $T_{\text{midpoint}}$  – midpoint temperature (the point at which the thermal degradation reaction is approx. half-way complete).

displayed slightly higher temperatures, aligning with those observed in the ceria groups, which recorded relatively higher values as compared to the control.

The mean and standard deviation ( $M \pm SD$ ) values for VH,  $\rho$  and Charpy IS for all groups, including the control group, are reported in Fig. 2–4. The experimental results

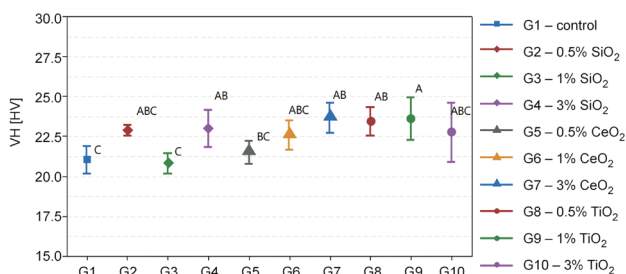


Fig. 2. Mean ( $M$ ) and standard deviation ( $SD$ ) values for Vickers hardness (VH) The  $SD$  values were used to calculate 95% confidence intervals ( $CIs$ ). Different letters in the graph show statistical differences between the groups ( $p < 0.05$ ; one-way ANOVA followed by Duncan's post hoc test).

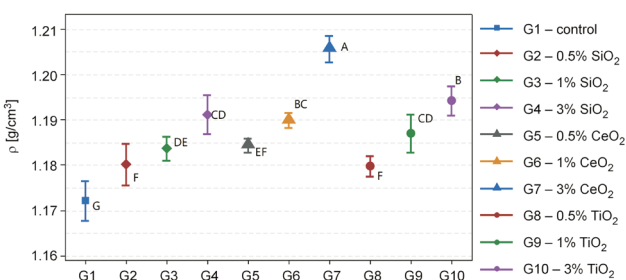


Fig. 3. Mean ( $M$ ) and standard deviation ( $SD$ ) values for density ( $\rho$ ) The  $SD$  values were used to calculate 95%  $CIs$ . Different letters in the graph show statistical differences between the groups ( $p < 0.05$ ; one-way ANOVA followed by Duncan's post hoc test).

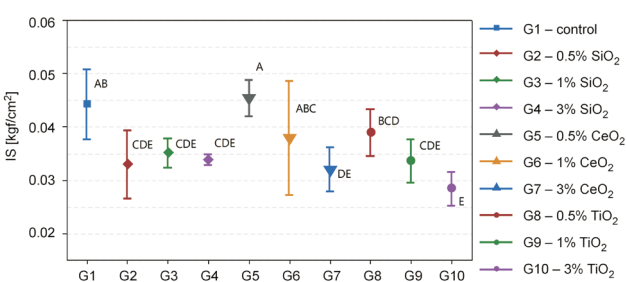


Fig. 4. Mean ( $M$ ) and standard deviation ( $SD$ ) values for impact strength (IS) The  $SD$  values were used to calculate 95%  $CIs$ . Different letters in the graph show statistical differences between the groups ( $p < 0.05$ ; one-way ANOVA followed by Duncan's post hoc test).

demonstrated significant variations in the mechanical properties among the different groups. Notably, the discernible differences in VH,  $\rho$  and IS could be attributed to variations in group composition. The one-way ANOVA revealed a statistically significant  $p$ -value ( $p < 0.05$ ), indicating the substantial influence of the NP content and concentration on the aforementioned mechanical properties, underscoring the importance of group composition in shaping the material characteristics.

The VH mean values for the control and 1% SiO<sub>2</sub> groups were significantly lower as compared to the 3% SiO<sub>2</sub>, 3% CeO<sub>2</sub>, 0.5% TiO<sub>2</sub>, and 1% TiO<sub>2</sub> groups (Fig. 2). Regarding density, the results show that the 3% CeO<sub>2</sub> group exhibited relatively higher scores, while the control group showed relatively lower values. The 0.5% SiO<sub>2</sub> and 0.5% TiO<sub>2</sub> groups had significantly lower means than the 3% TiO<sub>2</sub> group, though the results for the 3% SiO<sub>2</sub> and 1% TiO<sub>2</sub> groups did not differ statistically (Fig. 3). For IS, the mean values in the 3% TiO<sub>2</sub> group were significantly lower than those in the control, 0.5% CeO<sub>2</sub>, 1% CeO<sub>2</sub>, and 0.5% TiO<sub>2</sub> groups. The 3% CeO<sub>2</sub> group scores were lower than those in the 0.5% SiO<sub>2</sub>, 1% SiO<sub>2</sub>, 3% SiO<sub>2</sub>, 1% CeO<sub>2</sub>, 0.5% TiO<sub>2</sub>, and 1% TiO<sub>2</sub> groups, and significantly lower than those in the control, 0.5% CeO<sub>2</sub> and 1% CeO<sub>2</sub> groups (Fig. 4).

A comprehensive multiple two-way ANOVA yielded significant outcomes, further confirming the substantial impact of the NP weight percentage and type on the observed results. The specific details and outcomes of this analysis are succinctly presented in Table 2. With regard to VH, only the 1% TiO<sub>2</sub> group showed higher values. There were no significant differences among the NPs for the tested weight percentages within the range of 0.5 wt% and 3 wt%. Regarding the NP type, TiO<sub>2</sub> showed no differences when various weight percentages were used. For density, CeO<sub>2</sub> showed higher values; for all NP types, the density values increased along with the weight percentage. Moreover, CeO<sub>2</sub> displayed higher IS than SiO<sub>2</sub> and TiO<sub>2</sub>, which behaved similarly across all weight percentages. For SiO<sub>2</sub>, the lowest IS value was obtained for 0.5 wt%, and all types of NPs showed lower values when 3 wt% was incorporated, with no difference between 0.5 wt% and 1 wt%.

The fractographic examination verified that all samples could have FA and FB perfectly placed together, and not even the fracture line could be seen at  $\times 4$  magnification. Therefore, the fracture patterns were similar (Fig. 5).

Table 2. Multiple comparison analysis of the nanoparticle (NP) weight percentage (wt%) and type

Mechanical property	NP wt%			NP type		
	0.5%	1%	3%	SiO <sub>2</sub>	CeO <sub>2</sub>	TiO <sub>2</sub>
VH	Si = Ce = Ti	(Si = Ce) < Ti	Si = Ce = Ti	0.5% = 3% > 1%	0.5% = 1% = 3%	0.5% = 1% = 3%
$\rho$	Si = Ce = Ti	Si < Ce = Ti	Si < Ti < Ce	0.5% < (1% = 3%)	0.5% < 1% < 3%	0.5% < 1% < 3%
IS	(Si = Ti) < Ce	Si = Ce = Ti	Si = Ce = Ti	0.5% = 1% = 3%	(0.5% = 1%) > 3%	(0.5% = 1%) > 3%

VH – Vickers hardness;  $\rho$  – density; IS – impact strength; Si – silica; Ce – ceria; Ti – titania.

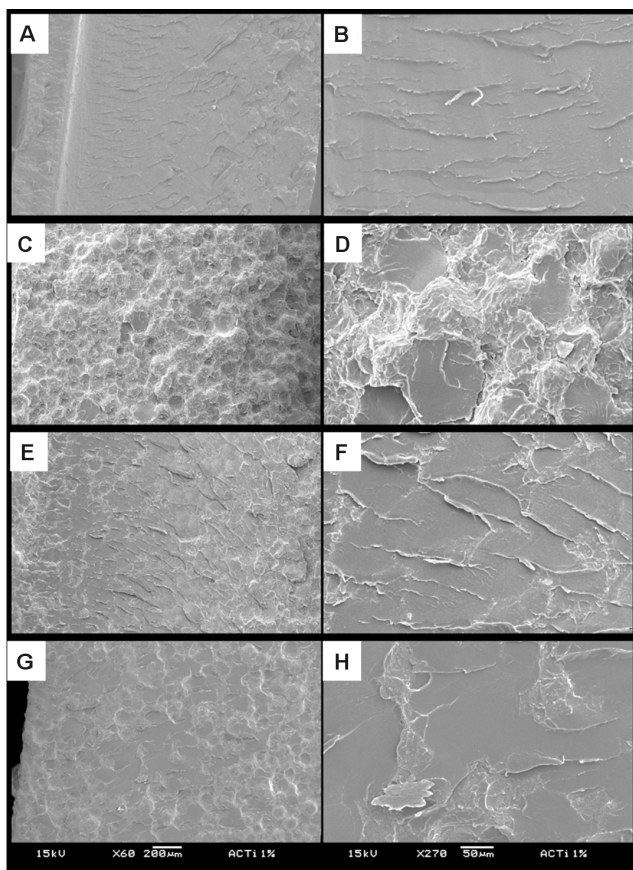


Fig. 5. Scanning electron microscopy (SEM) images of fracture topography with the incorporation of the nanoparticles (NPs) (1 wt%)

A – control (×60); B – SiO<sub>2</sub> (×60); C – CeO<sub>2</sub> (×60); D – TiO<sub>2</sub> (×60); E – control (×270); F – SiO<sub>2</sub> (×270); G – CeO<sub>2</sub> (×270); H – TiO<sub>2</sub> (×270).

## Discussion

The hypothesis for this study was rejected, since the incorporation of NPs into the acrylic resin altered all the tested properties. The concept of adding reinforcement materials to enhance the mechanical properties of a dental polymer is not novel.<sup>20</sup> Nanoscale fillers have a significantly greater surface area per mass unit than their larger versions, which can entirely change the way they interact with the polymer matrix. The filler particles used in this study were smaller (15–50 nm) than the resin powder particles (121.2 μm); thus, it was expected that they would fill the interstices between the particles of the polymer, forming a homogeneous mixture without forcing the displacement of the polymer chain segments.<sup>3,21</sup>

The percentage of particles was kept low so that all of them could be involved in the matrix. Increasing the percentage to 3% was expected to improve mechanical properties, as, theoretically, there would be less space between the oxide NPs. However, it has often proved difficult to achieve a stable dispersion of NPs in polymer matrices, as NPs tend to agglomerate.<sup>3,11,22</sup> The agglomerates can form stress concentration sites within the polymer matrix, leading to premature failure with the application

of load. Synthesizing the nanocomposite and separating the aggregated NPs were the main challenges of this study.

To disperse the NPs in the hydrophobic polymer matrix, the modification of the NP surfaces was required; it involved silanization and dual asymmetric centrifugal mixing processing.<sup>23</sup> Transmission electron microscopy was employed to characterize the uniformity, or lack thereof, of the NP dispersion in the resin matrix. Inorganic nanofillers were uniformly dispersed, more or less, when incorporated into the powder rather than the liquid. However, agglomeration could not be avoided, and the uniform dispersion throughout the polymer matrix was questionable (Fig. 1). Nonetheless, this could be explained by the suspected imbalance between depletion effects and osmotic pressures in PMMA, adversely impacting the fracture behavior.

Thermogravimetric analysis is a thermal analysis technique in which the mass variation of the sample (loss or gain) is determined as a function of temperature and/or time while the sample is subjected to a controlled temperature program.<sup>24</sup> Such changes are evidenced by a decrease or increase in mass registered by the sensor. Our TGA analysis presented 2 distinct events. The 1<sup>st</sup> event, at 175–330°C, could be related to the decomposition of secondary groups, such as the free CH<sub>3</sub> groups attached to the main polymer chain, generating volatiles. The 2<sup>nd</sup> and main mass loss event, at 328–455°C, can be attributed to the degradation of the main PMMA chain. As can be seen in Table 1, increases in the NP concentration and the NP content did not affect the initial degradation temperature (T<sub>i</sub>). The glass transition temperature is the temperature at which the movement of the polymer chain segments starts, and at which the material changes from a ‘glassy’ state (frozen) to a ‘rubber’ state (more flexible), which can be observed in the DSC curve. Since PMMA is an amorphous polymer, it showed a T<sub>g</sub> of approx. 105°C, as expected, which could be observed in the endothermic curve obtained in the heating run. Furthermore, we showed that the NPs may have interfered with the flowing process, which allows molecular chains to slide past each other, decreasing stiffness, and hence increased T<sub>g</sub>.<sup>25</sup> The incorporation of NPs showed satisfactory thermal stability for use in dental PMMA, since all types, depending on the weight percentage, exhibited degradation at a temperature comparable to that for the control group and a T<sub>g</sub> higher than in the control group.

The current study found that the incorporation of NPs increased microhardness, irrespective of the weight percentage, except for 1% SiO<sub>2</sub>. The different densities of the NPs interfere directly with the light weight of the acrylic resin, which can be desirable. In this study, the incorporation of NPs, regardless of their type and weight percentage, significantly increased the density of the resin. A low density can be partly associated with the formation of pores or microgaps, resulting from processing, a problem that affects acrylic resins for prostheses in general.

Such high-porosity-level sites facilitate fluid transport into and out of the polymer, serving as places for the sequestration of molecules.<sup>26</sup>

The NPs used in this study are insoluble in water and were meant to reduce the overall volume of the susceptible polymer matrix. Therefore, the higher density could be explained by a ‘packing’ effect, and not necessarily a lower porosity. In practice, impact fracture damage occurs when the patient accidentally drops the prosthesis. Studies have provided different proposals to minimize the susceptibility of the material to this flaw, such as increasing the thickness of the prosthesis in regions of increased susceptibility and modifying the matrix to improve the mechanical properties by adding polyfunctional agent crosslinks,<sup>27</sup> and the incorporation of a rubber phase,<sup>28</sup> fibers<sup>29</sup> and metal oxides.<sup>3</sup> Impact strength can be defined as the energy required to fracture a material under the impact force. In this study, IS was not affected by the NPs as much as the other properties. Most groups presented lower IS values than the control, which could be related to an increase in density, thus reducing stiffness.

Regarding IS, the groups that received SiO<sub>2</sub> showed very similar mechanical behavior, which might have been caused by the clustering of the NPs heterogeneously inside the PMMA matrix, resulting in weaker spots to propagate fractures. In this case, the incorporation of NPs into the polymer with a mixer seems to be insufficient to ensure a fully uniform dispersion of NPs. Further studies evaluating different methods should be developed to incorporate NPs into PMMA for dental and medical applications.

No cracks or missing material were observed under macroscopic evaluation. The A and B fragments of all samples could be placed together perfectly, suggesting that the NPs limited the crack propagation and kept the samples from breaking into several pieces. Some macro-phase separations could be observed in the silica and titania groups under SEM, while the ceria morphology was similar to that of the control group. The SEM images showed a honeycomb-like configuration for silica due to intense porosity, and compact and wave-like surfaces for the control or in the presence of ceria. The titania groups had both of these characteristics. Nanoparticles play a relevant role in polymerization configuration, and thus, in the fracture propagation patterns. A previous study used SEM to observe agglomeration in PMMA specimens containing 0.91% silica, and stated that the particles appeared to be embedded in and semi-bonded to the PMMA matrix, indicating a relatively strong NP–matrix interaction.<sup>30</sup> The present study corroborates this interaction pattern, though it was more visible in the ceria groups.

Balos et al. added nanosilica to the liquid component of a commercial PMMA-based resin, and found that it increased the microhardness and fracture toughness values for the lowest content.<sup>30</sup> Cerium oxide has been used in

dental materials to stabilize the polycrystalline tetragonal structure of zirconia.<sup>31</sup> To our knowledge, there are no reports of its use for acrylic resin reinforcement. Interestingly, in this study, CeO<sub>2</sub> NPs showed better overall behavior. In comparison with other groups containing NPs, the CeO<sub>2</sub> groups had a significantly higher degradation temperature, a higher mean IS, and similar VH and density values. Titanium oxide NPs are chemically inert, have a high refractive index and antibacterial properties under a variety of spectra, and are corrosion-resistant, non-toxic and inexpensive.<sup>14</sup> These NPs have been previously incorporated into polymeric materials, such as PMMA,<sup>15</sup> and were reported to provide better reinforcing properties than their micrometric version.<sup>16</sup> The impact of CeO<sub>2</sub> and TiO<sub>2</sub> on the resin color was readily apparent, potentially offering valuable insights. However, this effect should be given significant consideration in the evaluation and application of these NPs, warranting further in-depth investigation.

## Limitations

Some limitations of the current study are acknowledged. Firstly, the dispersion method should be refined, perhaps with the use of ultrasonication. Also, surface roughness analysis could be very useful for corroborating the hypothesis of increased wear resistance in two- and three-body wear, as well as when considering biofilm formation and biological aspects.<sup>32–34</sup>

## Conclusions

Incorporating all 3 types of NPs into the PMMA matrix significantly enhanced thermal stability, surface hardness and density. Moreover, the impact resistance in the tested NP groups remained comparable to that of the control group, indicating that modifying the microwave-cured acrylic resin with specific amounts of NPs, particularly CeO<sub>2</sub>, could serve as a viable solution to address the physico-chemical limitations of the material and to prevent unwanted clinical failure.

## Ethics approval and consent to participate

Not applicable.

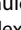
## Data availability

The datasets generated and/or analyzed during the current study are available from the corresponding author on reasonable request.

## Consent for publication

Not applicable.

## ORCID iDs

Luciana Machado-Santos  <https://orcid.org/0000-0001-5656-8760>  
 Kusai Baroudi  <https://orcid.org/0000-0002-1009-0869>  
 Nikolaos Silikas  <https://orcid.org/0000-0003-4576-4584>  
 João Paulo Mendes Tribst  <https://orcid.org/0000-0002-5412-3546>  
 Mario Alexandre Coelho Sinhoreti  <https://orcid.org/0000-0002-1932-2902>  
 William Cunha Brandt  <https://orcid.org/0000-0002-6297-6258>  
 Priscila Christiane Suzy Liporoni  <https://orcid.org/0000-0001-6787-1167>

## References

- Ladha K, Verma M. 19<sup>th</sup> century denture base materials revisited. *J Hist Dent*. 2011;59(1):1–11. PMID:21563724.
- Kawaguchi T, Lassila LV, Vallittu PK, Takahashi Y. Mechanical properties of denture base resin cross-linked with methacrylated dendrimer. *Dent Mater*. 2011;27(8):755–761. doi:10.1016/j.dental.2011.03.015
- Altaie SF. Tribological, microhardness and color stability properties of a heat-cured acrylic resin denture base after reinforcement with different types of nanofiller particles. *Dent Med Probl*. 2023;60(2):295–302. doi:10.17219/dmp/137611
- Raszewski Z. Acrylic resins in the CAD/CAM technology: A systematic literature review. *Dent Med Probl*. 2020;57(4):449–454. doi:10.17219/dmp/124697
- Zidan S, Silikas N, Alhotan A, Haider J, Yates J. Investigating the mechanical properties of ZrO<sub>2</sub>-impregnated PMMA nanocomposite for denture-based applications. *Materials (Basel)*. 2019;12(8):1344. doi:10.3390/ma12081344
- Souto Borges AL, De Oliveira Dal Piva AM, Moecke SE, De Moraes RC, Tribst JPM. Polymerization shrinkage, hygroscopic expansion, elastic modulus and degree of conversion of different composites for dental application. *J Compos Sci*. 2021;5(12):322. doi:10.3390/jcs5120322
- De Souza Leão R, Dantas de Moraes SL, De Luna Gomes JM, et al. Influence of addition of zirconia on PMMA: A systematic review. *Mater Sci Eng C Mater Biol Appl*. 2020;106:110292. doi:10.1016/j.msec.2019.110292
- Mitra SB, Wu D, Holmes BN. An application of nanotechnology in advanced dental materials. *J Am Dent Assoc*. 2003;134(10):1382–1390. doi:10.14219/jada.archive.2003.0054
- Wang H, Zhu M, Li Y, Zhang Q, Wang H. Mechanical properties of dental resin composites by co-filling diatomite and nanosized silica particles. *Mater Sci Eng C*. 2011;31(3):600–605. doi:10.1016/j.msec.2010.11.023
- Karabela MM, Sideridou ID. Synthesis and study of properties of dental resin composites with different nanosilica particles size. *Dent Mater*. 2011;27(8):825–835. doi:10.1016/j.dental.2011.04.008
- Slane J, Vivanco J, Ebenstein D, Squire M, Ploeg HL. Multiscale characterization of acrylic bone cement modified with functionalized mesoporous silica nanoparticles. *J Mech Behav Biomed Mater*. 2014;37:141–152. doi:10.1016/j.jmbbm.2014.05.015
- Fischer J, Stawarczyk B, Trottmann A, Hämmerle CH. Impact of thermal properties of veneering ceramics on the fracture load of layered Ce-TZP/A nanocomposite frameworks. *Dent Mater*. 2009;25(3):326–330. doi:10.1016/j.dental.2008.08.001
- Wang Q, Perez JM, Webster TJ. Inhibited growth of *Pseudomonas aeruginosa* by dextran- and polyacrylic acid-coated ceria nanoparticles. *Int J Nanomedicine*. 2013;8:3395–3399. doi:10.2147/IJN.S50292
- Reijnders L. The release of TiO<sub>2</sub> and SiO<sub>2</sub> nanoparticles from nanocomposites. *Polym Degrad Stab*. 2009;94(5):873–876. doi:10.1016/j.polymdegradstab.2009.02.005
- Chatterjee A. Effect of nanoTiO<sub>2</sub> addition on poly(methylmethacrylate): An exciting nanocomposite. *J App Polym Sci*. 2010;116(6):3396–3407. doi:10.1002/app.31883
- Shirkavand S, Moslehifard E. Effect of TiO<sub>2</sub> nanoparticles on tensile strength of dental acrylic resins. *J Dent Res Dent Clin Dent Prospects*. 2014;8(4):197–203. doi:10.5681/joddd.2014.036
- Acosta-Torres LS, López-Marín LM, Núñez-Anita RE, Hernández-Padrón G, Castaño VM. Biocompatible metal-oxide nanoparticles: Nanotechnology improvement of conventional prosthetic acrylic resins. *J Nanomater*. 2011;2011:941561. doi:10.1155/2011/941561
- Shibata S, Hirata I, Nomura Y, et al. Immobilization of simulated reducing agent at the surface of SiO<sub>2</sub> fillers in dental composite resins. *Dent Mater J*. 2007;26(4):568–574. doi:10.4012/dmj.26.568
- Sodagar A, Bahador A, Khalil S, Shahroudi AS, Kassaei MZ. The effect of TiO<sub>2</sub> and SiO<sub>2</sub> nanoparticles on flexural strength of poly (methyl methacrylate) acrylic resins. *J Prosthodont Res*. 2013;57(1):15–19. doi:10.1016/j.jpor.2012.05.001
- Paffenbager GC. Dental research at the National Bureau of Standards. *Science*. 1940;92(2397):527–528. doi:10.1126/science.92.2397.527
- Korkmaz T, Doğan A, Usanmaz A. Dynamic mechanical analysis of provisional resin materials reinforced by metal oxides. *Biomed Mater Eng*. 2005;15(3):179–188. PMID:15911998.
- Atai M, Pahlavan A, Moin N. Nano-porous thermally sintered nano silica as novel fillers for dental composites. *Dent Mater*. 2012;28(2):133–145. doi:10.1016/j.dental.2011.10.015
- Wilson KS, Antonucci JM. Interphase structure-property relationships in thermoset dimethacrylate nanocomposites. *Dent Mater*. 2006;22(11):995–1001. doi:10.1016/j.dental.2005.11.022
- Shakeri F, Nodehi A, Atai M. PMMA/double-modified organoclay nanocomposites as fillers for denture base materials with improved mechanical properties. *J Mech Behav Biomed Mater*. 2019;90:11–19. doi:10.1016/j.jmbbm.2018.09.033
- Bansal A, Yang H, Li C, Benicewicz BC, Kumar SK, Schadler LS. Controlling the thermomechanical properties of polymer nanocomposites by tailoring the polymer-particle interface. *J Polym Sci B Polym Phys*. 2006;44(20):2944–2950. doi:10.1002/polb.20926
- Panyayong W, Oshida Y, Andres CJ, Barco TM, Brown DT, Hovijitra S. Reinforcement of acrylic resins for provisional fixed restorations. Part III: Effects of addition of titania and zirconia mixtures on some mechanical and physical properties. *Biomed Mater Eng*. 2002;12(4):353–366. PMID:12652030.
- Vallo CI, Abraham GA, Cuadrado TR, San Román J. Influence of cross-linked PMMA beads on the mechanical behavior of self-curing acrylic cements. *J Biomed Mater Res B Appl Biomater*. 2004;70(2):407–416. doi:10.1002/jbm.b.30054
- Bettencourt AF, Neves CB, De Almeida MS, et al. Biodegradation of acrylic based resins: A review. *Dent Mater*. 2010;26(5):e171–e180. doi:10.1016/j.dental.2010.01.006
- Firmino AS, Tribst JPM, Nomura Nakano LJ, De Oliveira Dal Piva AM, Souto Borges AL, Arruda Paes-Junior TJ. Silica-nylon reinforcement effect on the fracture load and stress distribution of a resin-bonded partial dental prosthesis. *Int J Periodontics Restorative Dent*. 2021;41(2):e45–e54. doi:10.11607/prd.4347
- Balos S, Pilic B, Markovic D, Pavlicevic J, Luzanin O. Poly(methylmethacrylate) nanocomposites with low silica addition. *J Prosthet Dent*. 2014;111(4):327–334. doi:10.1016/j.prosdent.2013.06.021
- Yousefpour M, Askari N, Abdollah-Pour H, Amanzadeh A, Riahi N. Investigation on biological properties of dental implant by Ce-TZP/Al<sub>2</sub>O<sub>3</sub>/HA bio-nano-composites. *J Biotechnol Biomater*. 2011;1(2):105. doi:10.4172/2155-952X.1000105
- Jassim TK, Kareem AE, Alloaibi MA. In vivo evaluation of the impact of various border molding materials and techniques on the retention of complete maxillary dentures. *Dent Med Probl*. 2020;57(2):191–196. doi:10.17219/dmp/115104
- Gad MM, Fouda SM. Current perspectives and the future of *Candida albicans*-associated denture stomatitis treatment. *Dent Med Probl*. 2020;57(1):95–102. doi:10.17219/dmp/112861
- Possari JG, Mota Sacorague SC, Feitosa FA, Penteado MM, Bernardo Sichi LG, De Araújo RM. Influence of the addition of glass fibers reinforcements in the flexural strength of acrylic resin. *Braz Dent Sci*. 2020;23(3):1–5. doi:10.14295/bds.2020.v23i3.1955